JCI The Journal of Clinical Investigation

Peptide-conjugated oligonucleotides evoke long-lasting myotonic dystrophy correction in patient-derived cells and mice

Arnaud F. Klein, … , Denis Furling, Matthew J. A. Wood

J Clin Invest. 2019. https://doi.org/10.1172/JCI128205.

Concise Communication In-Press Preview

Antisense oligonucleotides (ASOs) targeting pathologic RNAs have shown promising therapeutic corrections for many genetic diseases including myotonic dystrophy (DM1). Thus, ASO strategies for DM1 can abolish the toxic RNA gain-of-function mechanism caused by nuclear-retained mutant transcripts containing CUG expansions (CUGexp). However, systemic use of ASOs for this muscular disease remains challenging due to poor drug distribution to skeletal muscle. To overcome this limitation, we test an arginine-rich Pip6a cell–penetrating peptide and show that Pip6a-conjugated morpholino phosphorodiamidate oligomer (PMO) dramatically enhanced ASO delivery into striated muscles of DM1 mice following systemic administration in comparison with unconjugated PMO and other ASO strategies. Thus, low-dose treatment of Pip6a-PMO-CAG targeting pathologic expansions is sufficient to reverse both splicing defects and myotonia in DM1 mice and normalizes the overall disease transcriptome. Moreover, treated DM1 patient–derived muscle cells showed that Pip6a-PMO-CAG specifically targets mutant CUGexp-DMPK transcripts to abrogate the detrimental sequestration of MBNL1 splicing factor by nuclear RNA foci and consequently MBNL1 functional loss, responsible for splicing defects and muscle dysfunction. Our results demonstrate that Pip6a-PMO-CAG induces high efficacy and long-lasting correction of DM1-associated phenotypes at both molecular and functional levels, and strongly support the use of advanced peptide-conjugates for systemic corrective therapy in DM1.

Peptide-conjugated oligonucleotides evoke long-lasting myotonic dystrophy correction in patient-derived cells and mice

Arnaud F. Klein[1†], Miguel A. Varela[2,3,4†], Ludovic Arandel[1], Ashling Holland[2,3,4], Naira Naouar[1], Andrey Arzumanov[2,5], David Seoane[2,3,4], Lucile Revillod[1], Guillaume Bassez[1], Arnaud Ferry[1,6], Dominic Jauvin[7], Genevieve Gourdon[1], Jack Puymirat[7], Michael J. Gait[5], Denis Furling[1#*] & Matthew J. A. Wood[2,3,4#*]

[1] Sorbonne Université, Inserm, Association Institut de Myologie, Centre de Recherche en Myologie, F-75013 Paris, France

[2] Department of Physiology, Anatomy and Genetics, University of Oxford, South Parks Road, Oxford, UK

[3] Department of Paediatrics, John Radcliffe Hospital, University of Oxford, Oxford, UK

[4] MDUK Oxford Neuromuscular Centre, University of Oxford, Oxford, UK

[5] Medical Research Council, Laboratory of Molecular Biology, Cambridge, UK.

[6] Sorbonne Paris Cité, Université Paris Descartes, Paris, France

[7] Unit of Human Genetics, Hôpital de l'Enfant-Jésus, CHU Research Center, QC, Canada

† These authors contributed equally to the work

# These authors shared co-last authorship

* To whom correspondence should be addressed to:

Matthew JA Wood
Department of Paediatrics
Le Gros Clark Building, South Parks Road,
Oxford, OX1 3QX, United Kingdom
Tel: +44(0)1865 282840
matthew.wood@paediatrics.ox.ac.uk

Denis Furling
Institute of Myology
Centre de Recherche en Myologie
47-83, bld de l'hôpital**,** 75013 Paris, France
Tel : +33 (0)1 42 16 57 07
denis.furling@sorbonne-universite.fr

Abstract

Antisense oligonucleotides (ASOs) targeting pathologic RNAs have shown promising therapeutic corrections for many genetic diseases including myotonic dystrophy (DM1). Thus, ASO strategies for DM1 can abolish the toxic RNA gain-of-function mechanism caused by nuclear-retained mutant *DMPK* transcripts containing CUG expansions (CUGexp). However, systemic use of ASOs for this muscular disease remains challenging due to poor drug distribution to skeletal muscle. To overcome this limitation, we test an arginine-rich Pip6a cell-penetrating peptide and show that Pip6a-conjugated morpholino phosphorodiamidate oligomer (PMO) dramatically enhanced ASO delivery into striated muscles of DM1 mice following systemic administration in comparison to unconjugated PMO and other ASO strategies. Thus, low dose treatment of Pip6a-PMO-CAG targeting pathologic expansions is sufficient to reverse both splicing defects and myotonia in DM1 mice and normalizes the overall disease-transcriptome. Moreover, treated DM1 patient derived muscle cells showed that Pip6a-PMO-CAG specifically targets mutant *CUGexp-DMPK* transcripts to abrogate the detrimental sequestration of MBNL1 splicing factor by nuclear RNA *foci* and consequently MBNL1 functional loss, responsible for splicing defects and muscle dysfunction. Our results demonstrate that Pip6a-PMO-CAG induces high efficacy and long-lasting correction of DM1-associated phenotypes at both molecular and functional levels, and strongly support the use of advanced peptide-conjugates for systemic corrective therapy in DM1.

Introduction

DM1, one of the most common muscular dystrophies in adults (1), is an RNA-dominant disorder caused by the expression of expanded microsatellite repeats located in the 3' untranslated region (UTR) of the *DMPK* gene (2-4). Mutant transcripts containing an expanded CUG tract are retained within the nucleus as discrete foci (5, 6). Due to the high affinity for CUGexp, RNA binding factors from the MBNL family are sequestered within the CUGexp-RNA *foci* leading to their functional loss (7), which is a central pathophysiologic mechanism in DM1 (8). Thus, altered splicing regulatory activity of MBNL1 in striated muscles results in many alternative splicing misregulations including those in *CLCN1*, *INSR*, *BIN1*, *DMD* and *SCN5A* pre-mRNAs that have been associated respectively with myotonia, insulin resistance, muscle weakness, dystrophic process and cardiac conduction defects, all symptoms of DM1 (9-14).

Given that the toxic RNA gain-of-function mechanism in DM1 is driven by pathologic CUGexp tract within *DMPK*-mRNAs, therapeutic approaches using modified ASOs aimed either to degrade CUGexp-transcripts using RNase H-active ASOs (15-17) or to release sequestered MBNL1 from CUGexp-RNAs using RNase H-inactive CAGn ASOs (18-20) have demonstrated efficient reversal of DM1-associated phenotypes. However, unlike other muscle diseases like Duchenne muscular dystrophy (DMD), the integrity of the skeletal muscle fiber membrane is not compromised in DM1 resulting in poor penetration of naked PMO- or 2'-O-methyl-ASOs (21). Backbone modifications led to the design of more potent chemistries including 2'-O-methoxyethyl or 2'-4'-constrained ethyl modified residues that enhanced ASO delivery and consequently therapeutic efficacy in skeletal muscles of DM1 mice(15, 17). This approach has been tested in a human clinical trial (NCT02312011); however systemic administration of the selected naked ASO did not achieve sufficient concentration levels in

skeletal muscle of patients to have marked clinical benefits. Therefore, tissue uptake remains a major challenge for ASO-therapies in DM1.

Among strategies to improve delivery of ASOs in DM1 skeletal muscles, cell-penetrating peptide conjugates offer an attractive avenue (22-24). Indeed, systemic administration of advanced Pip6a peptides conjugated with splice-switch oligonucleotides has shown promising results in DMD mice by restoring a truncated but functional dystrophin (25). Pip6a is a cell-penetrating peptide comprising a hydrophobic core region flanked on each side by arginine-rich domains containing β-alanine (B) and aminohexanoyl (X) spacers. This peptide sequence has the ability to deliver associated cargoes across the plasma and endosomal membranes and is stable to serum proteolysis (25). Here, we have investigated the potential of Pip6a conjugates to enhance RNase H-inactive CAGn-PMO delivery in skeletal muscles of DM1 mice in order to target nuclear-retained mutant CUGexp-transcripts and inhibit toxicity associated with expanded repeats.

Results / Discussion

To test whether advanced Pip6a conjugates enhanced ASO delivery and activity in skeletal muscles of DM1 mice following systemic administration, antisense PMOs composed of a CAG7 sequence, either naked (PMO) or conjugated to Pip6a peptide (Pip6a-PMO), were injected in the tail vein of HSA-LR mice. This well-characterized DM1 mouse model expresses 250 CTG repeats in the 3'UTR of the human skeletal muscle alpha actin (*HSA*) gene and displays molecular as well as functional DM1-associated abnormalities (26). The skeletal muscle-specific expression of CUGexp-RNAs in HSA-LR mice leads to the formation of ribonuclear foci that sequester MBNL1 proteins resulting in splicing defects and myotonia as found in DM1 patients (11, 27).

Two weeks after a single injection of a dose of 12.5 mg/kg, mice were sacrificed and the correction of DM1-splicing defects was used as a biomarker of ASO activity. Pip6a-PMO induced a partial but significant correction of several MBNL1-dependent splicing defects (e.g. *Clcn1 exon 7a*, *Mbnl1 exon 5* and *Atp2a1 exon 22*) in HSA-LR gastrocnemius muscle whereas no effect was observed with naked PMO at the same dose or even at a much higher dose of 200 mg/kg **(Figure 1A).** Moreover, two and three systemic injections of Pip6a-PMO (12.5 mg/kg) led respectively to an almost complete normalization and a full correction of DM1-splicing profiles of *Clcn1*, *Mbnl1* and *Atp2a1* genes in both HSA-LR gastrocnemius and quadriceps muscles **(Supplementary figure 1 and Figure 1B).** In contrast, even three injections of naked PMO at a high dose of 200 mg/kg did not improve splicing defects. PMO concentration was also quantified in skeletal muscle of HSA-LR mice by a custom ELISA assay. Results showed PMO concentrations of >1 nM two weeks after Pip6a-PMO treatment whereas mice treated with naked PMO showed low picomolar concentrations confirming the poor uptake of naked PMO in non-renal tissue **(Supplementary figure 2)**. Interestingly, systemic administration of Pip6a-PMO in DM1 mice leads also to therapeutic levels of PMO-CAG in heart and diaphragm

tissues that are affected in DM1 disease. Despite the restricted expression of CUGexp to the *hACTA1* gene in HSA-LR mice does not allow to assess ASO therapy in cardiac tissue, our results strongly suggest that the efficient biodistribution of Pip6a conjugated PMO into striated muscles could counteracted other DM1-related symptoms including cardiac conduction defects and respiratory failure, which are the most common causes of death in DM1 patients.

To determine whether Pip6a-PMO treatment can improve muscle function, we evaluated myotonia, a DM1 hallmark characterized by delayed muscle relaxation also detectable in HSA-LR mice. As shown in **Figure 1C-D**, Pip6a-PMO treatment completely abolished myotonia in gastrocnemius muscles of HSA-LR mice, which is in agreement with the correction of *Clcn1 exon 7a* missplicing responsible for myotonia (28). In contrast, systemic injections of a control Pip6a-PMO composed of a reverse GAC7 sequence (Pip6a-Ctrl) had no effect on either DM1-splicing defects or myotonia in HSA-LR mice (**Supplementary figure 3A-B).** Altogether these results showed that a low-dose treatment of Pip6a conjugates allows efficient systemic delivery of ASO in skeletal muscle of DM1 mice. Remarkably, optimal beneficial effects at both molecular and functional levels were achieved with a cumulative dose of Pip6a-ASO that is five to ten times lower than either unconjugated or conjugated-ASOs previously described and evaluated in the same DM1 mouse model (15, 17, 22, 29).

To examine the overall effect of Pip6a-PMO on the skeletal muscle transcriptome of DM1 mice, we performed a deep paired-end RNA sequencing. The principal component analysis (PCA) showed that gene expression in the gastrocnemius muscle of HSA-LR mice treated with Pip6a-PMO was shifted towards WT mice (**Figure 2A)**. Moreover, the heatmap performed with all the transcripts having a significant change (n=3176; adj. p-value<0.1; no threshold in fold change (FC)) confirmed the global gene expression correction in treated HSA-LR mice (**Figure 2B**). Strikingly, the vast majority (85%) of the most significant changes observed at the gene expression level in HSA-LR mice (FC≥2 and adj. p-values<0.1; 376 transcripts) were corrected

in treated mice with an average correction index of 76% (**Figure 2C and Supplementary table 1)**. In addition, most of the deregulated genes containing CTG repeats ≥7 in skeletal muscles were also corrected in treated HSA-LR mice (**Supplementary table 2**). Transcriptomic analysis confirmed also that Pip6a-PMO treatment induced a global correction of alternative splicing misregulation measured in HSA-LR mice (adj. p-value<0.1; no threshold in FC; **Figure 2D**). Thus 80% of the most deregulated splicing events in HSA-LR mice (FC≥2 and adj. p-values<0.1; 339 events) were normalized in treated mice an average correction index of 83% (**Figure 2E**) also leading to correction of the deregulated biological pathways **(Supplementary figure 4 and Supplementary table 3).** Similar results were obtained from the quadriceps muscle of the same treated-mice (**Supplementary figure 5)** indicating that the muscle transcriptome of DM1 mice could be almost normalized by Pip6a-PMO treatment targeting pathologic CUGexp. In addition, PCA and heatmap analysis (FC≥ 1.5; p-value <0.05; n=118) of the proteome assessed by label-free mass spectrometry revealed that protein expression in the quadriceps muscle of treated HSA-LR mice also tends to shift from a disease towards a wild type profile, supporting the correction of the DM1 muscle phenotype by Pip6a-PMO treatment (**Supplementary figure 6 and Supplementary table 4**).

To further determine the consequences of Pip6a-PMO on CUGexp-RNA behavior, we examined nuclear RNA foci number and CUGexp-RNA levels since it has been shown previously that both features were reduced by RNase H-inactive CAGn-antisense-ASOs (18, 19). Likewise, a similar mechanism of action, which is not yet fully explained, was also observed in Pip6a-PMO treated HSA-LR mice as i) missplicing reversal due to the release of functional MBNL1 from CUGexp-RNA foci was associated with a 50% reduction in the number of myonuclei containing RNA foci in treated muscles (**Figure 3A-B and Supplementary figure 7**); ii) a 60% decrease of CUGexp-RNA steady-state levels was

detected following Pip6a-PMO treatment whereas control Pip6a-Ctrl treatment had no effect on CUGexp-RNA expression (**Figure 3C and Supplementary figure 3C**).

Besides, the duration of Pip6a-PMO action in HSA-LR skeletal muscles was evaluated because activity and beneficial effect of nuclease-resistant ASOs could be maintained for several weeks *in vivo* (15, 30-32). Correction of splicing changes was used as a molecular biomarker and Pip6a-PMO effect was assessed up to six months post-treatment. As observed in **Figure 3D**, splicing misregulation of *Clcn1 exon 7a*, *Mbnl1 exon 5* and *Atp2a1 exon 22* pre-mRNAs were completely normalized in both HSA-LR gastrocnemius and quadriceps muscles until four weeks after systemic administration. Moreover, a significant 80 to 100% of correction of these splicing defects was still measured twenty-six weeks post-treatment supporting a long-lasting activity of Pip6a-PMO, which remained nearly complete for a six-month period. Furthermore, mild histological changes observed in liver or kidney two weeks after Pip6a-PMO injections were mostly reversed six months later (**Supplementary table 5**) supporting transient and reversible side effects of Pip6a-PMO treatment.

Finally, molecular effects of Pip6a-PMO were assessed in human DM1 muscle cells carrying a large expansion (2600 repeats) and expressing within its natural context both mutant *CUGexp-DMPK* and non-mutated *normal-DMPK* transcripts (33). Pip6a-PMO treatment induced the displacement and relocation of MBNL1 from RNA foci towards the nucleoplasm as observed in WT muscle cells (**Figure 4A)**. Moreover, MBNL1-dependent splicing defects of *LDB3*, *MBNL1*, *SOS1* and *DMD* pre-mRNAs that are present in DM1 differentiated muscle cells were significantly corrected by Pip6a-PMO confirming the functional restoration of MBNL1 *(***Figure 4B**). Similar results were obtained in another DM1 cell line carrying >1300CTG and described previously (33) (**Supplementary Figure 8**). Importantly, no splicing changes were observed neither in DM1 muscle cells treated with Pip6a-Ctrl or naked PMO nor in WT muscle cells treated with Pip6a-PMO (**Supplementary Figure 9**). As a consequence of MBNL1

displacement from CUGexp-RNA foci, Pip6a-PMO treatment induced a 79% decrease in the number of foci per nucleus associated with an 40% increase in the number of nucleus without foci (**Figure 4C-D**), which was consistent with a 77% decrease of CUGexp-*DMPK* transcript levels in treated DM1 cells (**Figure 4E-F**). A direct measurement of CUGexp-*DMPK* transcripts using single molecule RNA FISH also confirmed the reduced level of *CUGexp-DMPK* mRNA by Pip6a-PMO treatment in muscle cells expressing the human *DMPK* gene with 1500CTG (**Supplementary figure 10**). Remarkably, products of non-mutated *DMPK* alleles were not affected in DM1-treated cells supporting a specific targeting of Pip6a-PMO composed of a CAG7 sequence to mutant *DMPK* transcripts containing CUGexp tract (**Figure 4E-F**).

In conclusion, our study demonstrates that Pip6a cell-penetrating-peptide improves the penetration of ASO in striated muscles of DM1 mice after systemic delivery. Thus, low dose treatment of Pip6a-conjugated PMO directed against pathogenic CUGexp repeats is sufficient to achieve an effective concentration of ASO in muscle fibers and induces an efficient and long-lasting correction of molecular and functional phenotypes in DM1 mice. Altogether these results strongly support the development of ASO-conjugates peptides for further clinical trial in DM1 as well as other microsatellite expansion disorders.

Methods

See the supplemental Methods for a full description of all experimental procedures.

Statistics. All group data are expressed as mean +/- SEM. Comparisons were performed by Mann-Whitney test or one-way ANOVA test followed by Newman-Keuls or Tukey post-test using Prism6 software (GraphPad Software, Inc.). Differences between groups were considered significant when $P \leq 0.05$.

Study approval. Experiments on HSA-LR mice were carried out according to French legislation and Ethics committee approval (#1760-2015091512001083v6).

Data availability. Complete raw data generated from RNA sequencing were deposited in the Gene Expression omnibus database (GEO ; GSE134926).

Author contribution

Experiments were performed by A.F.K, M.A.V, L.A, A.H, D.S, A.F, L.R, and D.J. A.A produced the Pip6a-PMO. Transcriptomic analysis was performed by N.N. Proteomics data were generated and analyzed by A.H. Data were analyzed by A.F.K, M.A.V, G.B, G.G, J.P, M.J.G, M.J.W and D.F. The study was designed and written by M.J.A.W and D.F. As part of a joint collaborative work, co-first and co-last authors order was decided to ensure both teams have equitable representation.

Acknowledgements

This work was supported by the Association Francaise contre les Myopathies/AFM-Telethon (grant 15758), Association Institut de Myologie, Muscular Dystrophy UK (16GRO-PG36-0091), Medical Research Council (MR/P01741X/1) and the John Fell Fund (152/058). We would like to thank Mégane Lemaitre from the Muscle Function Evaluation platform (UMS28), and C. Thornton for the MBNL1 polyclonal antibody and the HSA^{LR} mouse model.

Competing financial interest

M.J.G. and M.J.W are co-founders of PepGen, a company committed to the enhanced peptide delivery of oligonucleotide therapeutics for treatment of neuromuscular and other diseases.

References

1. Harper PS. *Myotonic dystrophy*. London: W.B. Saunders - Harcourt Publishers; 2001:

2. Mahadevan M et al. Myotonic dystrophy mutation: an unstable CTG repeat in the 3' untranslated region of the gene. *Science* 1992;255(5049):1253–1255.

3. Brook JD et al. Molecular basis of myotonic dystrophy: expansion of a trinucleotide (CTG) repeat at the 3' end of a transcript encoding a protein kinase family member. *Cell* 1992;68(4):799–808.

4. Fu YH et al. An unstable triplet repeat in a gene related to myotonic muscular dystrophy. *Science* 1992;255(5049):1256–1258.

5. Taneja KL, McCurrach M, Schalling M, Housman D, Singer RH. Foci of trinucleotide repeat transcripts in nuclei of myotonic dystrophy cells and tissues. *J Cell Biol* 1995;128(6):995–1002.

6. Davis BM, McCurrach ME, Taneja KL, Singer RH, Housman DE. Expansion of a CUG trinucleotide repeat in the 3' untranslated region of myotonic dystrophy protein kinase transcripts results in nuclear retention of transcripts. *Proc Natl Acad Sci USA* 1997;94(14):7388–7393.

7. Miller JW et al. Recruitment of human muscleblind proteins to (CUG)(n) expansions associated with myotonic dystrophy. *EMBO J* 2000;19(17):4439–4448.

8. Lee K-Y et al. Compound loss of muscleblind-like function in myotonic dystrophy. *EMBO Mol Med* 2013;5(12):1887–1900.

9. Savkur RS, Philips AV, Cooper TA. Aberrant regulation of insulin receptor alternative splicing is associated with insulin resistance in myotonic dystrophy. *Nat Genet* 2001;29(1):40–47.

10. Charlet-B N et al. Loss of the muscle-specific chloride channel in type 1 myotonic dystrophy due to misregulated alternative splicing. *Molecular Cell* 2002;10(1):45–53.

11. Mankodi A et al. Expanded CUG repeats trigger aberrant splicing of ClC-1 chloride channel pre-mRNA and hyperexcitability of skeletal muscle in myotonic dystrophy. *Molecular Cell* 2002;10(1):35–44.

12. Rau F et al. Abnormal splicing switch of DMD's penultimate exon compromises muscle fibre maintenance in myotonic dystrophy. *Nat Commun* 2015;6(1):385–10.

13. Freyermuth F et al. Splicing misregulation of SCN5A contributes to cardiac-conduction delay and heart arrhythmia in myotonic dystrophy. *Nat Commun* 2016;7:11067.

14. Fugier C et al. Misregulated alternative splicing of BIN1 is associated with T tubule alterations and muscle weakness in myotonic dystrophy. *Nat. Med.* 2011;17(6):720–725.

15. Wheeler TM et al. Targeting nuclear RNA for in vivo correction of myotonic dystrophy. *Nature* 2012;488(7409):111–115.

16. Lee JE, Bennett CF, Cooper TA. RNase H-mediated degradation of toxic RNA in myotonic dystrophy type 1. *Proc. Natl. Acad. Sci. U.S.A.* 2012;109(11):4221–4226.

17. Jauvin D et al. Targeting DMPK with Antisense Oligonucleotide Improves Muscle Strength in Myotonic Dystrophy Type 1 Mice. *Molecular Therapy: Nucleic Acid* 2017;7:465–474.

18. Wheeler TM et al. Supp-Reversal of RNA Dominance by Displacement of Protein Sequestered on Triplet Repeat RNA. *Science* 2009;325(5938):336–339.

19. Mulders SAM et al. Triplet-repeat oligonucleotide-mediated reversal of RNA toxicity in myotonic dystrophy. *Proc. Natl. Acad. Sci. U.S.A.* 2009;106(33):13915–13920.

20. Wojtkowiak-Szlachcic A et al. Short antisense-locked nucleic acids (all-LNAs) correct alternative splicing abnormalities in myotonic dystrophy. *Nucleic Acids Res.* 2015;43(6):3318–3331.

21. González-Barriga A et al. Cell membrane integrity in myotonic dystrophy type 1: implications for therapy. *PLoS ONE* 2015;10(3):e0121556.

22. Leger AJ et al. Systemic Delivery of a Peptide-Linked Morpholino Oligonucleotide Neutralizes Mutant RNA Toxicity in a Mouse Model of Myotonic Dystrophy. *Nucleic Acid Therapeutics* 2013;23(2):109–117.

23. Lehto T, Ezzat K, Wood MJA, Andaloussi El S. Peptides for nucleic acid delivery. *Advanced Drug Delivery Reviews* 2016;106(Pt A):172–182.

24. McClorey G, Banerjee S. Cell-Penetrating Peptides to Enhance Delivery of Oligonucleotide-Based Therapeutics. *Biomedicines* 2018;6(2):51.

25. Betts C et al. Pip6-PMO, A New Generation of Peptide-oligonucleotide Conjugates With Improved Cardiac Exon Skipping Activity for DMD Treatment. *Molecular Therapy: Nucleic Acid* 2012;1:e38.

26. Mankodi A et al. Myotonic Dystrophy in Transgenic Mice Expressing an Expanded CUG Repeat. *Science* 2000;289(5485):1769–1772.

27. Lin X et al. Failure of MBNL1-dependent post-natal splicing transitions in myotonic dystrophy. *Human Molecular Genetics* 2006;15(13):2087–2097.

28. Wheeler TM, Lueck JD, Swanson MS, Dirksen RT, Thornton CA. Correction of ClC-1 splicing eliminates chloride channelopathy and myotonia in mouse models of myotonic dystrophy. *J. Clin. Invest.* 2007;:1–6.

29. Sobczak K, Wheeler TM, Wang W, Thornton CA. RNA Interference Targeting CUG Repeats in a Mouse Model of Myotonic Dystrophy. *Molecular Therapy* 2013;21(2):380–387.

30. Wu B et al. Long-term rescue of dystrophin expression and improvement in muscle pathology and function in dystrophic mdx mice by peptide-conjugated morpholino. *Am. J. Pathol.* 2012;181(2):392–400.

31. Miller CM, Harris EN. Antisense Oligonucleotides: Treatment Strategies and Cellular Internalization. *RNA Dis* 2016;3(4). doi:10.14800/rd.1393

32. Rinaldi C, Wood MJA. Antisense oligonucleotides: the next frontier for treatment of neurological disorders. *Nat Rev Neurol* 2018;14(1):9–21.

33. Arandel L et al. Immortalized human myotonic dystrophy muscle cell lines to assess therapeutic compounds. *Dis Model Mech* 2017;10(4):487–497.

Figures legends:

Figure 1: Pip6a-PMO corrects molecular and functional defects in HSA-LR mice. HSA-LR mice were injected with single or multiple doses of naked PMO-CAG7 (PMO) or Pip6a-PMO-CAG7 (Pip6a-PMO) by intravenous injection and analyzed 2 weeks after treatment. **A)** Quantification of splicing correction induced by single 12.5 mg/kg dose of Pip6a-PMO, 12.5 or 200 mg/kg dose of PMO in gastrocnemius of treated mice (WT n=4; HSA-LR n=10; PMO n=4; Pip6a-PMO n=6). **B)** Representative RT-PCR results and quantification of alternative splicing profiles in gastrocnemius (gast.) and quadriceps (quad.) of HSA-LR mice treated with three injections of PMO at 200 mg/kg or Pip6a-PMO at 12.5 mg/kg (WT n=7; HSA-LR n=16; PMO n=4; Pip6a-PMO n=8). **C)** Representative maximal force/time curves obtained by *in situ* force measurements of Pip6a-PMO treated mice (3x12.5 mg/kg) compared to WT and HSA-LR mice. **D)** Correction of myotonia (measured as the area under the force/time curve during relaxation after maximal muscle contraction) in Pip6a-PMO injected HSA-LR mice (WT n=6; HSA-LR n=7; Pip6a-PMO n=8). *Data are expressed as mean +/- SEM, except for D: box 25-75th percentile; whiskers min to max; black line indicates the mean. Statistics: One-way ANOVA with Newman-Keuls post-test; *, P<0.05; **, P<0.01; ***, P<0.001*; *****, P<0.0001; n.s., non-significant.*

Figure 2: Treatment with Pip6a-PMO normalizes global transcriptome at both expression and splicing levels. Transcriptomic analysis by RNA sequencing was performed on total RNA isolated from gastrocnemius muscles of treated HSA-LR mice compared to HSA-LR and WT mice (n=3). **A-B)** Principal component analysis (A) and heatmap graphic (B) of all significantly expressed transcripts (adj. p-value>0.1) reveal a global correction of genes expression profile with Pip6a-PMO treatment. **C)** Global correction of gene expression by Pip6a-PMO treatment

(n=376; FC≥2, adj. p-value<0.1): 85.5% of transcripts return to FC<2 with an average correction index of 76%; 8% of transcripts remains at FC≥2 but with correction index >20%; 6.5% of transcripts are not corrected. **D)** Heatmap graphic of all significant deregulated exon_bin (normalized counts) reveals a global correction of missplicing events with Pip6a-PMO treatment. **E)** Overall correction of alternative splicing profiles by Pip6a-PMO treatment (n=339 splicing events; FC≥2, adj. p-value<0.1): 80% of events return to FC<2 with an average correction index of 83%; 11% remains at FC≥2 but with correction index>20%; 8% are not corrected.

Figure 3: Treatment with Pip6a-PMO normalizes DM1-specific phenotype. HSA-LR mice were injected in tail vein with three 12.5 mg/kg doses of Pip6a-PMO and analyzed 2 weeks after treatment. **A)** Representative pictures of gastrocnemius muscle section stained for CUGexp-foci (FISH, red), fibers membrane (WGA, grey) and nucleus (Hoechst, blue) (scale bar : 50µm). **B)** Quantification of the number of nuclei with foci in gastrocnemius muscle sections (HSA-LR n=7; Pip6a-PMO n=8). **C)** Quantification of HSA transcripts levels by qRT-PCR (HSA-LR n=12; Pip6a-PMO n=8). **D)** Quantification of splicing correction in gastrocnemius (gast.) and quadriceps (quad.) at 2 weeks, 4 weeks and 6 months after treatment (HSA-LR n=16; n=4 for each time point of Pip6a-PMO). *Data are expressed as mean +/- SEM. Statistics B: Mann-Whitney test; C and D: One-way ANOVA with Newman-Keuls post-test; *, P<0.05; **, P<0.01; ***, P<0.001; n.s., non-significant.*

Figure 4: Pip6a-PMO corrects DM1-specific molecular symptoms in DM1 muscle cells. Four days differentiated immortalized DM1 myoblasts (2600 CTG repeats) are treated with Pip6a-PMO at 1 µM and analyzed after 24h. **A)** Combined FISH (Cy3-CAG, red) /immuno-fluorescence (MBNL1, green) on DM1 or WT differentiated myoblasts (scale bar : 10 µm). **B)**

Quantification of splicing corrections by RT-PCR (WT n=4; DM1 and Pip6a-PMO n=7). **C)** Quantification of mean number of foci per nucleus in treated DM1 differentiated myoblasts (n=4; >500 nucleus per n). **D** Quantification of the number of nucleus without foci in treated DM1 differentiated myoblasts (n=4; >500 nucleus per n). **E-F)** Levels of *mutDMPK*/*normDMPK* transcripts analyzed by Northern blot using a *DMPK* probe (n=4). *Data are expressed as mean +/- SEM. Statistics: B and F: One-way ANOVA with Newman-Keuls post-test; C and D: Mann-Whitney test; *, P<0.05; **, P<0.01; ***, P<0.001; ****, P<0.0001; n.s., non-significant.*

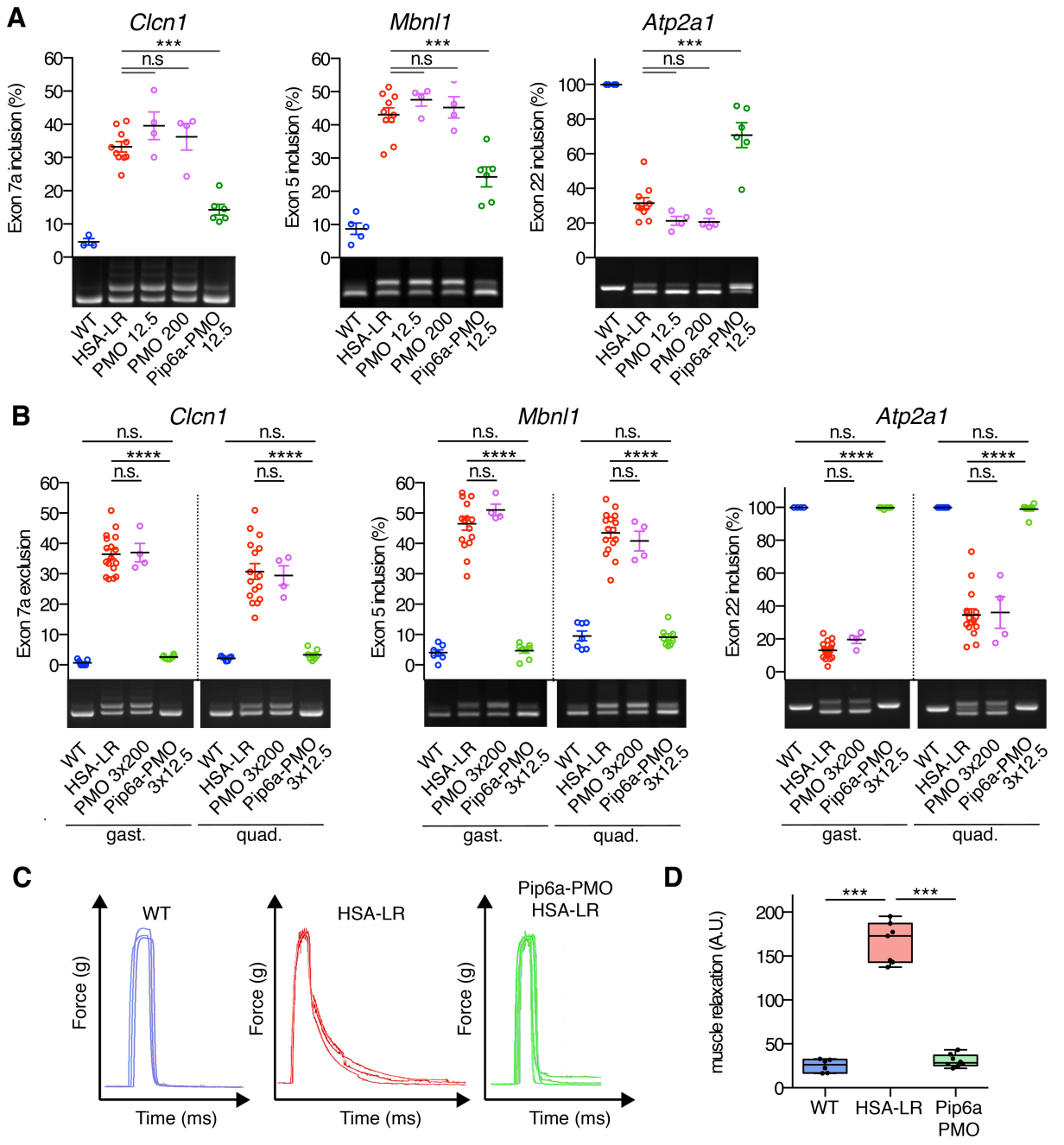

Figure 1: Pip6a-PMO corrects molecular and functional defects in HSA-LR mice. HSA-LR mice were injected with single or multiple doses of naked PMO-CAG7 (PMO) or Pip6a-PMO-CAG7 (Pip6a-PMO) by intravenous injection and analyzed 2 weeks after treatment. **A)** Quantification of splicing correction induced by single 12.5 mg/kg dose of Pip6a-PMO, 12.5 or 200 mg/kg dose of PMO in gastrocnemius of treated mice (WT n=4; HSA-LR n=10; PMO n=4; Pip6a-PMO n=6). **B)** Representative RT-PCR results and quantification of alternative splicing profiles in gastrocnemius (gast.) and quadriceps (quad.) of HSA-LR mice treated with three injections of PMO at 200 mg/kg or Pip6a-PMO at 12.5 mg/kg (WT n=7; HSA-LR n=16; PMO n=4; Pip6a-PMO n=8). **C)** Representative maximal force/time curves obtained by *in situ* force measurements of Pip6a-PMO treated mice (3x12.5 mg/kg) compared to WT and HSA-LR mice. **D)** Correction of myotonia (measured as the area under the force/time curve during relaxation after maximal muscle contraction) in Pip6a-PMO injected HSA-LR mice (WT n=6; HSA-LR n=7; Pip6a-PMO n=8). *Data are expressed as mean +/- SEM, except for D: box 25-75th percentile; whiskers min to max; black line indicates the mean. Statistics: One-way ANOVA with Newman-Keuls post-test; *, P<0.05; **, P<0.01; ***, P<0.001; ****, P<0.0001; n.s., non-significant.*

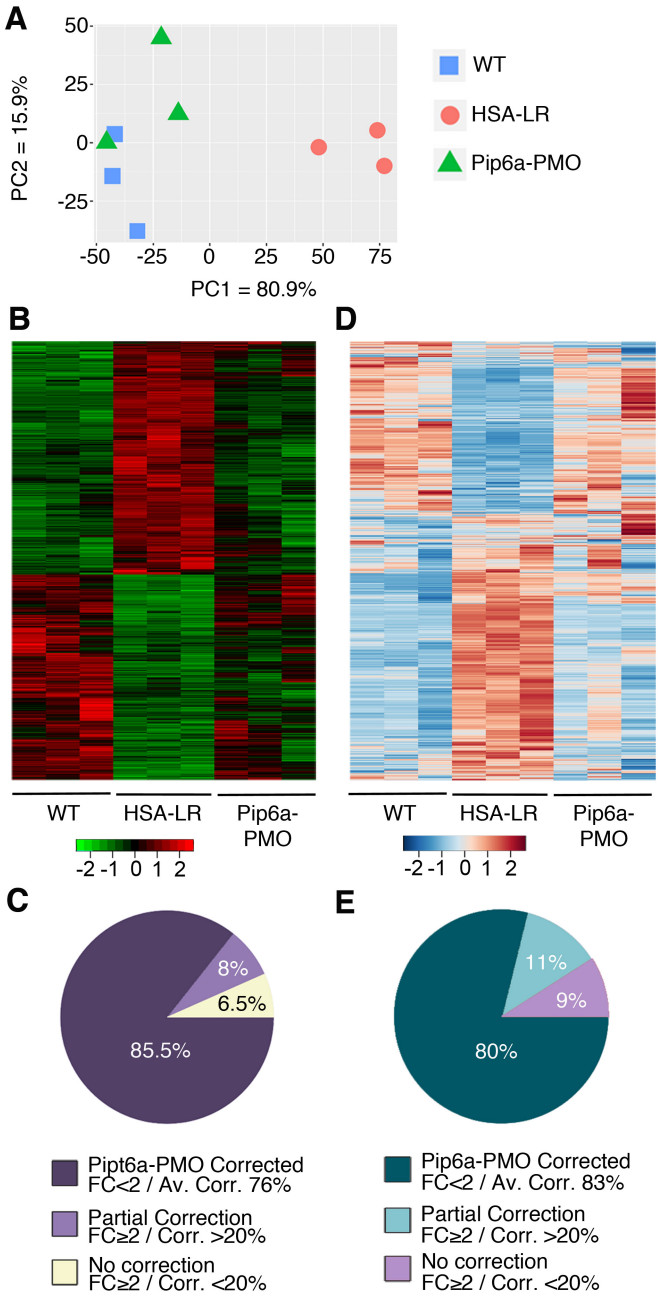

Figure 2: Treatment with Pip6a-PMO normalizes global transcriptome at both expression and splicing levels. Transcriptomic analysis by RNA sequencing was performed on total RNA isolated from gastrocnemius muscles of treated HSA-LR mice compared to HSA-LR and WT mice (n=3). **A-B)** Principal component analysis (A) and heatmap graphic (B) of all significantly expressed transcripts (adj. p-value>0.1) reveal a global correction of genes expression profile with Pip6a-PMO treatment. **C)** Global correction of gene expression by Pip6a-PMO treatment (n=376; FC≥2, adj. p-value<0.1): 85.5% of transcripts return to FC<2 with an average correction index of 76%; 8% of transcripts remains at FC≥2 but with correction index >20%; 6.5% of transcripts are not corrected. **D)** Heatmap graphic of all significant deregulated exon_bin (normalized counts) reveals a global correction of missplicing events with Pip6a-PMO treatment. **E)** Overall correction of alternative splicing profiles by Pip6a-PMO treatment (n=339 splicing events; FC≥2, adj. p-value<0.1): 80% of events return to FC<2 with an average correction index of 83%; 11% remains at FC≥2 but with correction index>20%; 8% are not corrected

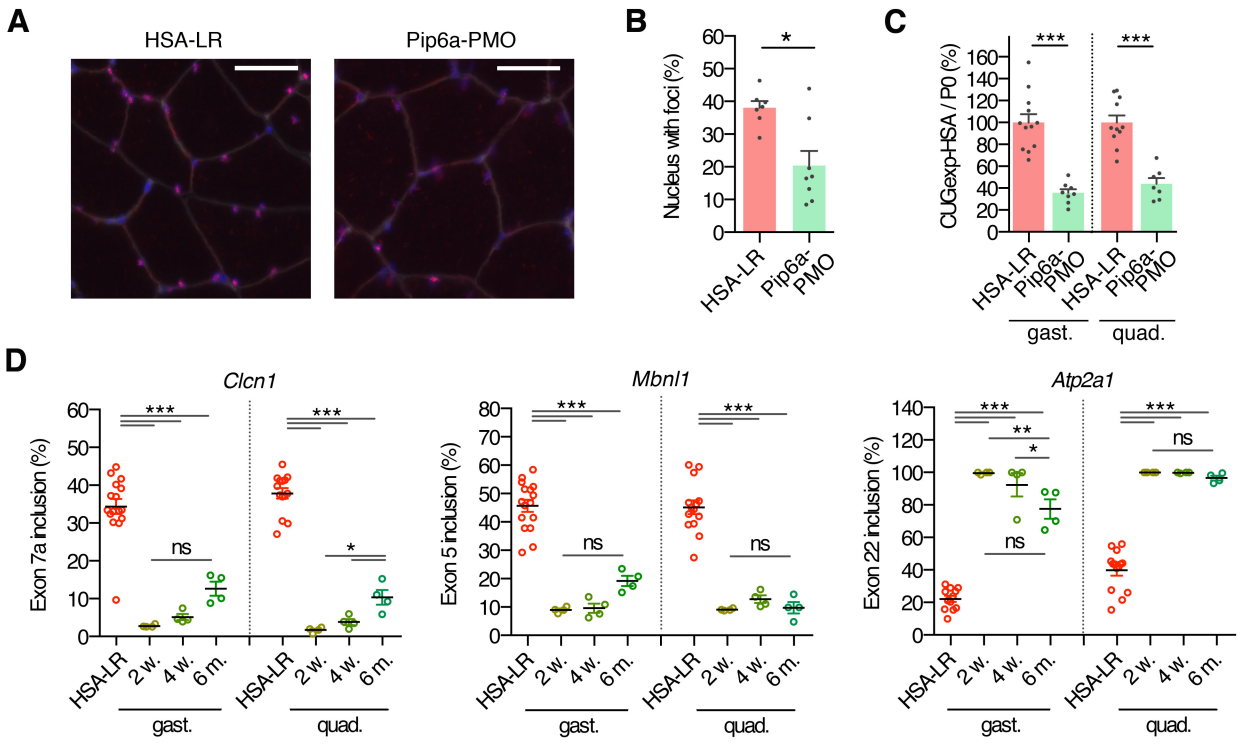

Figure 3: Treatment with Pip6a-PMO normalizes DM1-specific phenotype. HSA-LR mice were injected in tail vein with three 12.5 mg/kg doses of Pip6a-PMO and analyzed 2 weeks after treatment. **A)** Representative pictures of gastrocnemius muscle section stained for CUGexp-foci (FISH, red), fibers membrane (WGA, grey) and nucleus (Hoechst, blue) (scale bar : 50μm). **B)** Quantification of the number of nuclei with foci in gastrocnemius muscle sections (HSA-LR n=7; Pip6a-PMO n=8). **C)** Quantification of HSA transcripts levels by qRT-PCR (HSA-LR n=12; Pip6a-PMO n=8). **D)** Quantification of splicing correction in gastrocnemius (gast.) and quadriceps (quad.) at 2 weeks, 4 weeks and 6 months after treatment (HSA-LR n=16; n=4 for each time point of Pip6a-PMO). *Data are expressed as mean +/- SEM. Statistics B: Mann-Whitney test; C and D: One-way ANOVA with Newman-Keuls post-test; *, P<0.05; **, P<0.01; ***, P<0.001; n.s., non-significant.*

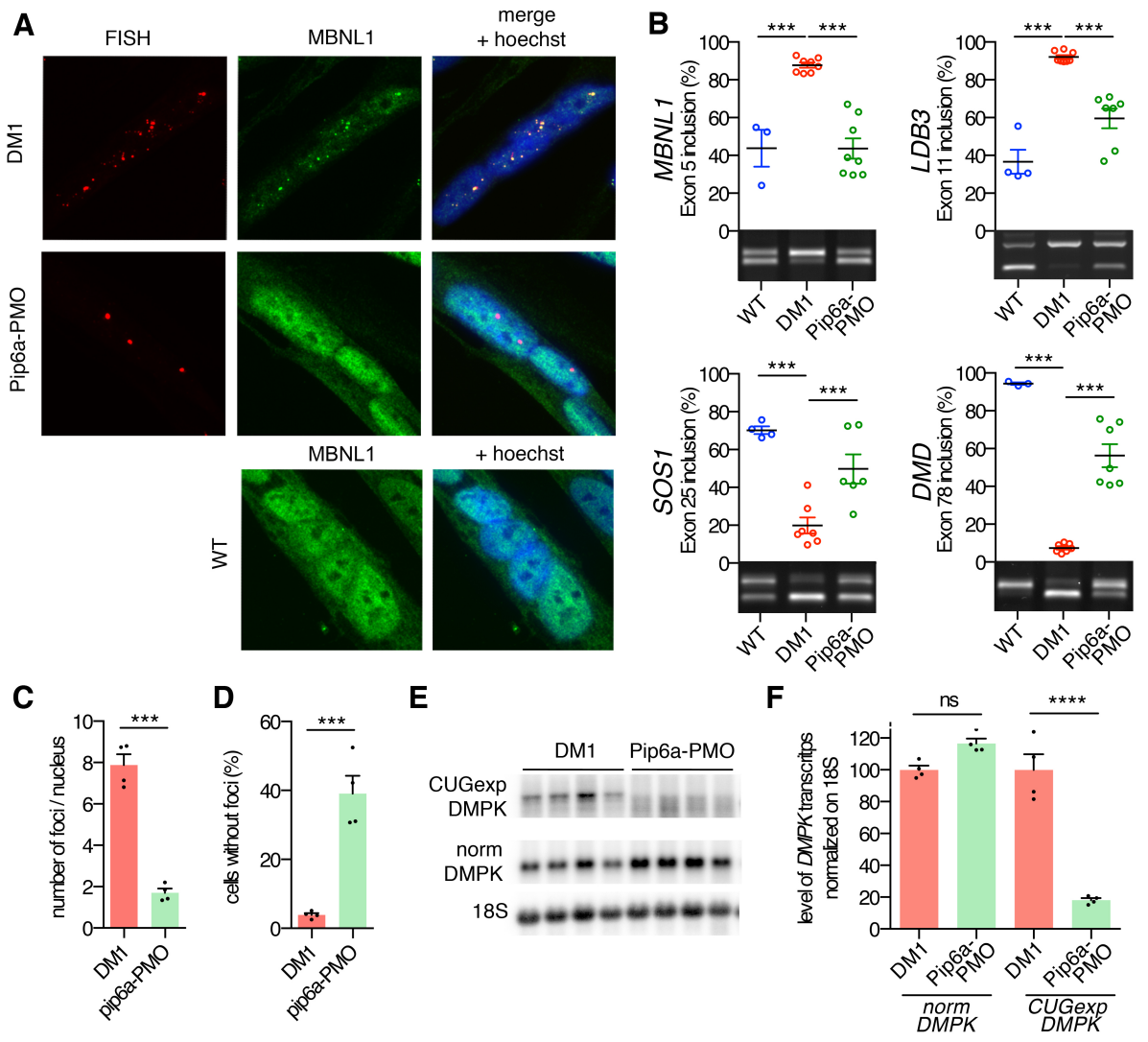

Figure 4: Pip6a-PMO corrects DM1-specific molecular symptoms in DM1 muscle cells. Four days differentiated immortalized DM1 myoblasts (2600 CTG repeats) are treated with Pip6a-PMO at 1 μM and analyzed after 24h. **A)** Combined FISH (Cy3-CAG, red) /immuno-fluorescence (MBNL1, green) on DM1 or WT differentiated myoblasts (scale bar : 10 μm). **B)** Quantification of splicing corrections by RT-PCR (WT n=4; DM1 and Pip6a-PMO n=7). **C)** Quantification of mean number of foci per nucleus in treated DM1 differentiated myoblasts (n=4; >500 nucleus per n). **D** Quantification of the number of nucleus without foci in treated DM1 differentiated myoblasts (n=4; >500 nucleus per n). **E-F)** Levels of *mutDMPK*/*normDMPK* transcripts analyzed by Northern blot using a *DMPK* probe (n=4). *Data are expressed as mean +/- SEM. Statistics: B and F: One-way ANOVA with Newman-Keuls post-test; C and D: Mann-Whitney test; *, P<0.05; **, P<0.01; ***, P<0.001; ****, P<0.0001; n.s., non-significant.*